Chapter 1

INTRODUCTION

1.1 GENERAL

The determination of the ultimate bearing capacity of a shallow foundation is a well-known classical problem in geotechnical engineering. There are several analytical and numerical techniques that are used to find the bearing capacity of soil. They are limit equilibrium method, variational method, method of stress characteristics (slip line method), elastoplastic finite element method, finite difference method, limit analysis based (rigid block-based as well as finite-element based) method. Owing to the advancement of the finite element method and different robust optimization techniques, the finite element limit analysis (FELA) has emerged as a very powerful tool for solving various stability problems in geomechanics. For the past few decades, researchers have been using this method to solve many foundation problems (Lysmer, 1970; Anderheggen and Knopfel, 1972; Bottero et al., 1980; Pastor and Turgeman, 1982; Sloan, 1988, 1989; Sloan and Kleeman, 1995: Lyamin and Sloan, 2002a, 2002b; Makrodimopoulos and Martin, 2006, 2007; Merifield et al., 2006; Krabbenhoft et al., 2007; Kumar and Khatri, 2011). The main advantages of the finite element limit analysis technique over other numerical and analytical techniques are listed below:

(a) The FELA technique does not require any assumptions regarding the slip surface or the collapse mechanism.

(b) All the inherent benefits of the finite element method are retained in FELA indicating that the FELA technique can deal with complicated boundary conditions, arbitrary geometries, inherent and stress-dependent heterogeneities, and anisotropies.

(c) Unlike the displacement-based finite element method, the FELA technique predicts the collapse load without performing any step-by-step elastoplastic analysis. Thus, the computational effort reduces significantly without any need for a complete constitutive model.

(d) The FELA technique provides a rigorous solution as it fulfills all three basic tenets of the mechanics of deformable solids: the stress equilibrium conditions, the strain displacement equations, and the stress-strain relationships.

In this thesis, the FELA technique has been suitably modified and explicitly used for addressing the axisymmetric problems in saturated soils and plane strain problems in unsaturated soils. The following sections briefly describe the limit analysis and the basic tenets of unsaturated soil mechanics.

1.2 LIMIT ANALYSIS

The limit analysis is based on the theory of plasticity and brackets the true solution within two extremities by using the following two theorems:

(a) Lower bound limit theorem (Drucker et al. 1951)

"*If a stress distribution (σ_{ij}) can be found which satisfies equilibrium equations, balances the applied tractions T_i on the traction boundary A_T and nowhere violates the yield condition $f(\sigma_{ij}) \leq 0$, then the traction T_i and the body forces F_i will be less than, or equal to, the actual traction and body forces that cause collapse.*"

(b) Upper bound limit theorem (Drucker et al. 1951)

"*If a compatible plastic deformation field comprised of velocity field and strain-rate field can be found which satisfies the velocity boundary condition along the boundary and the normality condition, then the tractions T_i and the body forces F_i*

determined by equating the rate of external work done to the rate of dissipation of an internal energy will be greater than, or equal to, the actual collapse load comprised of tractions and body forces."

The stress field which adheres to the basic requirements of the lower bound theorem (i.e. obeying stress equilibrium equations, stress boundary conditions, and yield criterion) is regarded as the "statically admissible stress (SAS) field". The velocity field which adheres to the basic requirement of the upper bound theorem (i.e., obeying strain-displacement relationship, velocity boundary conditions, normality rule) is regarded as the "kinematically admissible velocity (KAV) field". The lower and the upper bound collapse loads are the maximum and the minimum collapse loads that are generated by the SAS and the KAV fields, respectively.

In contrast to the plane strain problems, there are limited works in the field of axisymmetric problems. Kumar and Khatri (2011) proposed an axisymmetric lower bound limit analysis by forcibly imposing the Haar and Von-Karman (1909) hypothesis that relates the hoop stress (σ_θ) with the principal stresses during plastic deformation. The Haar-von Karman hypothesis (1909) states that depending on the soil's stress path, the circumferential stress, σ_θ, in an axisymmetric stability problem can be equated either with the major (when the soil undergoes active stress state) or the minor (when the soil undergoes active stress state) principal stress. Without imposing any restrictions on σ_θ, Salgado et al. (2004) and Lyamin et al. (2007) solved the axisymmetric problem with the aid of three-dimensional (3D) FELA. Nevertheless, it is quite evident that the complexities associated with the 3D elements are enormous. In view of these complexities, in the present thesis, an axisymmetric lower bound formulation has been employed based on two-dimensional finite elements and three-dimensional yield criterion. The shape of the chosen yield surfaces, namely, Mohr-Coulomb (for drained

sands), Tresca (for undrained clays), and Hoek-Brown yield surfaces, appears to be hexagonal pyramid, hexagonal prism, and hexagonal curved-edged pyramids respectively, in the three-dimensional stress invariant plane. The apex of the Mohr-Coulomb and Hoek-Brown yield pyramids and the vertices of all the hexagonal yield surfaces possess sharp stress discontinuities. During the computational process, constructing the gradient vectors and the Hessian matrices with the usage of the original yield criterion with sharp corners becomes problematic. Following Sloan and Booker (1986), Abbo and Sloan (1995), and Abbo et al. (2011), the yield criteria are sufficiently smoothened by using the hyperbolic approximation in the meridian plane and the trigonometric round-off technique in the octahedral plane. The smoothening process eventually turns the chosen yield surfaces to be C^2 continuous, and thereby, a unique value of first- and second-order derivatives is guaranteed at any point on the yield surface. Owing to the nature of the yield constraint, the convex optimization problem becomes nonlinear. The interior point method based on the logarithmic barrier function is employed for solving the nonlinear optimization problem. In this numerical iteration process, the search direction and the step sizes are chosen by reducing the barrier parameter at each iteration until it reaches zero at the optimum point. The smoothened yield surfaces are subsequently used to address a few unsolved problems of ring footings.

1.3 BASIC TENENTS OF UNSATURATED SOIL MECHANICS (USM)

Fredlund (1996) estimated that approximately 60% of the world's population lived in arid and semiarid climatic conditions, which constitutes approximately 33% (Vanapalli and Oh, 2010) of the earth's surface. In these climatic regions, the groundwater table lies at a considerable depth from the natural ground surface.

Therefore, the soils from the ground surface to a few meters deep are partially saturated. Due to the development of tensile forces in the unsaturated medium, the strength and stiffness of the unsaturated soil become significantly higher than its saturated counterpart. While predicting the ultimate bearing capacity of soils, if the degree of saturation is not properly incorporated in the analysis, the resulting solutions could be highly conservative, and eventually, the design cost will increase.

Unlike saturated soil mechanics, which is derived from two-phase soil systems (either air-solids or water-solid), unsaturated soil mechanics is primarily based on three phases: air, water, and solids. Later, Fredlund and Morgenstern (1977) perceived the existence of a fourth phase in the unsaturated soil. This additional phase is the air-water interface, designated as the contractile skin. It behaves as an elastic membrane and brings the soil particles into closer proximity by virtue of surface tension. Contrary to the saturated mechanics, pore air and contractile skin strongly influence the vadose zone's mechanical properties. Conventionally, pore-air pressure is used as a reference for the development of two independent stress state variables (Fredlund and Morgenstern, 1977; Matyas and Radhakrishna, 1968; Fredlund and Rahardjo, 1993), namely, net normal stress ($\sigma - u_a$) and matric suction ($\psi = u_a - u_w$); σ, u_a, and u_w are the total normal stress, pore-air, and pore-water pressures, respectively. It is to be noted that the presence of matric suction establishes the demarcation of saturated and unsaturated soils. Since the pore-air pressure frequently encountered in the field is atmospheric, the matric suction can be explained as a negative pore-water pressure relative to the pore-air pressure. Changes in the water content directly impact the matric suction. The lower the water content, the higher the matric suction. When matric suction increases, the contractile skin exerts a tensional strain on the soil particle, increasing the soil's shear strength (Wijaya and Leong, 2016). The change in the water content, or, in other words,

the variation in matric suction influences the resistance to the water flow. The main determinants of the vertical distribution of matric suction in unsaturated soil are the various environmental factors, encompassing rainfall, relative humidity, solar radiation, evaporation, as well as vegetation, human activities like gardening and car washing, and the location of the groundwater table. These factors work together to produce the various matric suction profiles depicted in Figure 1.1.

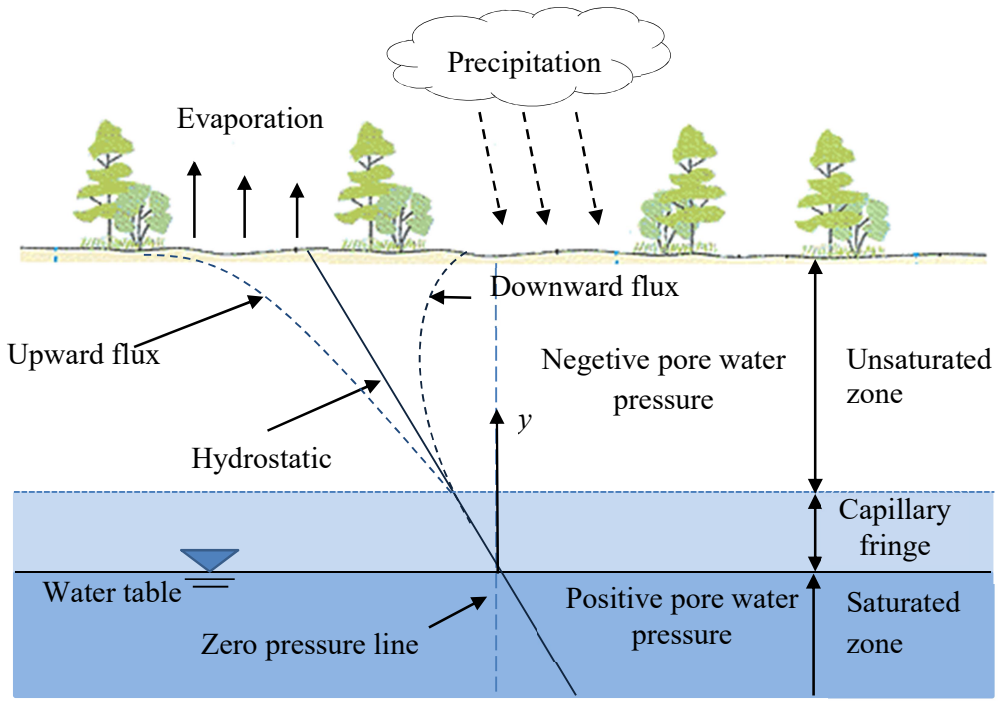

Figure 1.1 The variation of matric suction profiles in the unsaturated zone

If there is no water flow, the matric suction profile remains linear. On the other hand, the flow of water in the vadose zone creates nonlinear matric suction profiles. The upward flux results in high matric suction, whereas the downward flux reduces the matric suction at the ground surface (Fredlund et al., 2012; Jeong et al., 2017). The relation between the water content and the matric suction is the most powerful tool in dealing with unsaturated soils. This relationship has been pivotal in expanding the scope

of saturated soil mechanics by embracing and incorporating the complexities of unsaturated soil behaviour. The following section talks about that relationship in detail.

1.3.1 Soil-Water Retention Curve

In geotechnical engineering, the linkage between the water volume and the matric suction is described through the *soil water retention curve*, abbreviated as SWRC. The water volume can be represented as gravimetric water content (w), volumetric water content (θ), or degree of saturation (S). Compared to other fields, such as soil physics and agricultural engineering, incorporating SWRC curves into real-life geotechnical problems is a relatively recent development. These disciplines have long been familiar with the curve, commonly identified as the water retention or soil potential curve. The SWRC considers the key stress state variable and serves as the single most important interpretive and predictive tool to understand the strength behaviour of soil, its deformational characteristics related to volume changes, water distribution in the voids, and the flow characteristics exhibited within the soil. Typical soil-water characteristic curves in terms of $\theta-\psi$ and $S-\psi$ are displayed in Figure 1.2. The graph represents two nonlinear curves: (a) main drying or desorption (solid line) curve, and (b) main wetting or adsorption (dashed line) curve. Due to the high range of matric suction (the matric suction window may vary from 10^{-4}–10^{6} kPa), the curves are plotted in the semi-logarithmic graph. Based on the thermodynamic relationship between the soil suction and partial pressure of water vapour (Gibbs free-energy state equation) demonstrate that the maximum soil suction is approximately 10^{6} kPa. The SWRC indicates the reduction of water content with the increasing matric suction and is hysteretic in nature. An increase in matric suction characterizes the drying phase, whereas the wetting phase is associated with a reduction in matric suction. The hysteresis in the SWRC curve refers to a non-unique relationship between the soil's

matric suction and water content. It indicates that at the same matric suction, the water contents will be estimated differently from the drying and the wetting curve. Thus, the retained water is a function of the drying and wetting history of the soil. Figure 1.2 depicts the three separate zones of the drying SWRC curve: boundary effect zone, transition zone, and residual zone.

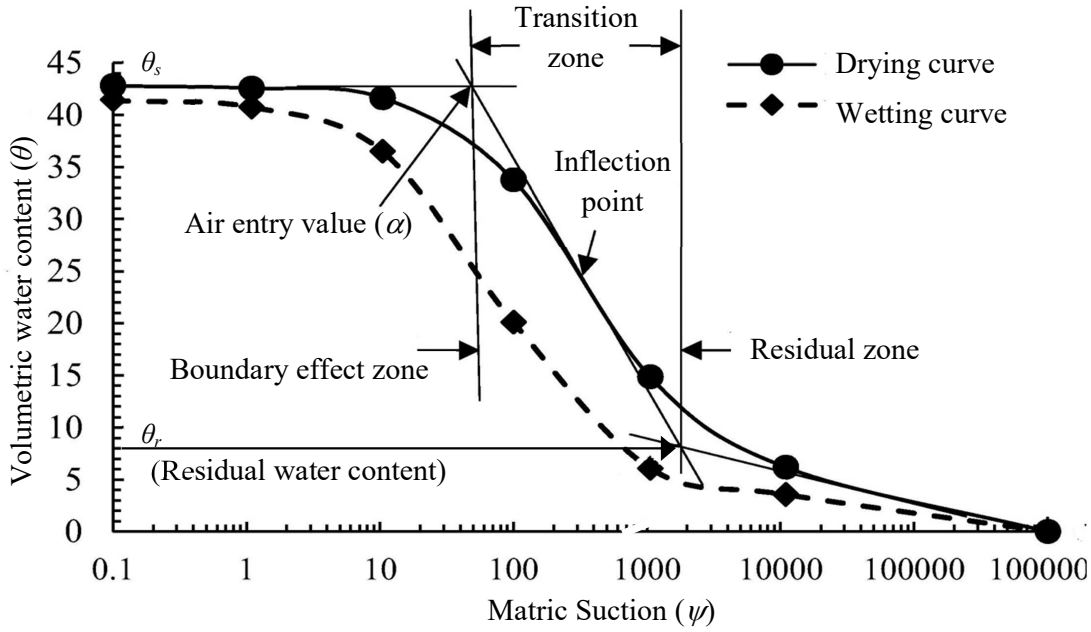

Figure 1.2 Typical features of the soil–water retention curve (modified after Vanapalli et al. (1996)

The boundary effect zone is the capillary fringe zone where the soil possesses matric suction but is completely saturated. In this zone, the water phase is continuous, but the air phase is discontinuous (air is present in occluded form). After the end of this zone, the soil enters the transition zone where both the fluid phases (air and water) are continuous. This zone exhibits the maximum fraction of desaturation. At higher matric suction, soil attains the residual state where the reduction in water content with respect to the matric suction is minimal. Generally, researchers believe that after arriving at the residual state, liquid flow essentially ceases, and vapour flow dominates over the

moisture flow. Along the SWRC, two well-defined, distinct points delineate the boundaries of these three zones. These are the air entry value (AEV) and the residual water content. The AEV is the matric suction beyond which the air recedes into the soil's pores, and the desaturation process commences during the drying phase. For the progression of desaturation, the matric suction value must exceed the AEV. The fine-grained soil's AEV is substantially higher than the coarse-grained soil. The residual water content is the water content where a larger suction is required to extract additional water from the soil. A tangent line drawn through the inflection point intersects the back-propagated lines from the saturated and residual states and generates the AEV and residual water content, respectively. Notably, the drying SWRC and the wetting SWRC curves result in different fitting parameters. For the sake of computational simplicity, in the present study, the SWRC fitting parameters are idealized to be unaffected by the compaction energy, hysteresis effect, number of wetting-drying cycles, stress state, initial dry density, and initial water content.

A good number of mathematical models are prescribed (Gardner, 1958; Brooks and Corey, 1964; van Genuchten, 1980; Fredlund and Xing, 1994; Kosugi, 1994; Pereira and Fredlund, 2000) for approximating the SWRC primarily based on the (a) onset of desaturation, (b) rate of desaturation, and (c) realization of the residual condition. Brooks and Corey (1964, 1966) and Jeppson (1974) developed an analytical expression for SWRC based on Burdine's theory (1953). However, their proposed expression introduced a discontinuity in the slopes of both the SWRC and the unsaturated hydraulic conductivity curve, particularly at a negative pressure head value known as the bubbling pressure. This discontinuity posed challenges, hindering rapid convergence in numerical simulations of saturated-unsaturated flow and thereby reducing the accuracy of their equation. Subsequently, van Genuchten (1980), Fredlund,

and Xing (1994) introduced a three-parameter equation capable of improved SWRC simulation across the entire suction range from 0 to 10^6 kPa. van-Genuchten (1980) model (vG SWRC) is one of the most widely used SWRC models with a closed-form equation to map the nonlinearity between soil suction and the volumetric water content. Fredlund and Xing (1994) refined the SWRC model by incorporating a correction factor, extending the suction range to completely dry conditions beyond the soil's residual suction limit, aligning with realistic experimental results. Through a comprehensive evaluation, Leong and Rahardjo (1997) concluded that both van-Genuchten (1980) and Fredlund and Xing (1994) equations offered superior fits across diverse soil conditions. Owing to its simplicity, reversibility, computational flexibility, and wide usage, the vG SWRC model is employed in the present thesis to describe the relationship between water content and matric suction for a steady-state water flow. Further the flow in the vdose zone is assumed to be governed by Gardner's (1958) one-parameter hydraulic conductivity function (HCF), and Darcy's linear flow law. The impact of the model parameters are elaborately presented in Chapter 7.

1.3.1.1 van-Genuchten SWRC model (1980)

According to the vG SWRC model, the water content (or degree of saturation) and the matric suction are related as follows:

$$\Theta_n = S_e = \left\{ \frac{1}{1+\left[\alpha\left(u_a - u_w\right)\right]^n} \right\}^m \tag{1.1}$$

where, (a) $\Theta_n \left(= \frac{\theta - \theta_r}{\theta_s - \theta_r} \right)$ and $S_e \left(= \frac{S - S_r}{1 - S_r} \right)$ are the normalized water content and effective degree of saturation, respectively; here, (i) θ_r and θ_s are the residual- and saturated water content, respectiveely, and (ii) S_r is the residual degree of saturation.

(b) α, n, and m are the fitting parameters of the van-Genuchten SWRC curve; α^{-1}, in a way, reflects the inverse of air entry value, n is the dimensionless pore spectrum number, and m controls the sigmoidal shape of the SWRC curve. The magnitude of α and n varies between 0.001 to 0.5 kPa^{-1} and 1.1 to 8.5 (Lu and Likos, 2004), respectively. Based on the steady-state suction profiles, Lu and Griffith (2004) extensively examined the limiting values of Q and n for different regimes; the lowering limit of n was shown as 1.1.

1.3.2 Gardner's Hydraulic Conductivity Function (1958)

Due to its simplicity, the hydraulic conductivity of the unsaturated soil is assumed to be dictated by Gardner's (1958) one-parameter hydraulic conductivity function as described below:

$$k = k_s e^{-\alpha(u_a - u_w)} \tag{1.2}$$

where, k_s = saturated hydraulic conductivity. This equation depicts that the hydraulic conductivity of a variably saturated zone decays exponentially with the matric suction.

1.3.3 Flow Law

The flow within the vadose zone is considered to be one-dimensional (vertical), steady-state, and governed by Darcy's linear flow law (q= ki); here, q = steady-state flow rate, k= matric suction-dependent unsaturated hydraulic conductivity function, and i is the total head gradient. Neglecting osmotic, electrical, thermal, and velocity heads, the hydraulic head (combination of matric suction and elevation heads) becomes the fundamental driving potential for water flow. Hence, Darcy's law turns out to be:

$$q = k\left(\frac{d(u_a - u_w)}{\gamma_w dy} + 1\right) \tag{1.3}$$

Here, (i) q is termed as the specific discharge rate of steady-state flow in the vertical direction; the magnitude of q can be negative, zero, or positive depending upon the flow

conditions, i.e., infiltration, no-flow, and evaporation, respectively. (ii) y represents the height above the water table (as shown in Figure 1.1), and (iii) γ_w is the unit weight of water.

1.3.4 Effective stress

The usage of matric suction is the building block of performing stability analysis of the partially saturated soil. By using these two independent stress state variables, namely, net normal stress $(\sigma - u_a)$ and matric suction $(\psi = u_a - u_w)$, Bishop (1959) pioneered in proposing the definition of effective stress for unsaturated soils:

$$\sigma' = (\sigma - u_a) + \chi (u_a - u_w) \tag{1.4}$$

Here, χ is the saturation-state-dependent single-valued effective stress parameter which lies between 0 (for completely dry) and 1(for completely saturated) and reflects the matric suction contribution towards the effective stress. However, Bishop's effective stress concept failed to predict the mechanical responses observed in unsaturated soils during wetting. Jennings and Burland's (1962) conducted oedometer tests on air-dry samples and demonstrated that the single effective stress approach could not represent the wetting-induced collapse compression under constant total stress. A few other researchers (Bishop and Blight, 1963; Burland, 1965; Matyas and Radhakishna, 1968; and Brackley, 1971) also raised these doubts. Since then, many researchers (Kohgo et al., 1993; Modaressi and Abou-Bekr, 1994; Bolzon et al., 1996; Loret and Khalili, 2000; Khalili and Loret, 2001) demonstrated the effectiveness of effective stress in explaining plastic deformation of unsaturated soils. Khalili et al. (2004) extensively reviewed the early studies and provided experimental validation of the effective stress principle in unsaturated soil mechanics.

Following the effective stress principle and the conventional Mohr-Coulomb failure criterion, the shear strength of the unsaturated soil was described as:

$$\tau = c' + (\sigma - u_a)\tan\phi' + \chi(u_a - u_w)\tan\phi' \quad (1.5a)$$

$$= c' + (\sigma - u_a)\tan\phi' + (u_a - u_w)\tan\phi^b \quad ; \quad \tan\phi^b = \chi\tan\phi' \quad (1.5b)$$

It is to be noted that in this equation, all the stress state parameters are measured at the failure state. Here, c' represents the cohesion at zero matric suction, ϕ' is the internal friction angle associated with the net normal stress, and ϕ^b is an internal friction angle that characteries the rise in shear strength with respect to the matric suction. In this context, note that cohesion and friction represent the intercept and slope angle of the linear MC yield envelope. The efficacy of these shear strength equation was earlier verified through a series of triaxial tests (Fredlund et al., 1978; Sheng at al., 2009; Kim and Borden, 2011). Several other researchers (Gan et al., 1988; Escario and Juca 1989; Vanapalli et al., 1996) had earlier demonstrated through substantial experimental evidence that the angle, ϕ^b, is a highly nonlinear function of matric suction; in the boundary effect zone $\phi^b = \phi'$, thereafter ϕ^b starts reducing and can be as low as 0° or even negative when ψ approaches towards the residual saturation state. Figure 1.3a shows the curvilinear failure profile in the three-dimensional stress plane (τ–(σ–u_a)–ψ).

Although Equation (1.5b) is quite a celebrated and widely used approach for estimating the shearing strength of soil in the vadose zone, however, Prof. Lu and his coworkers demonstrated that the following serious concerns strictly inhibit the use of these two parameters (χ and ψ) separately:- (a) the difficulties and uncertainties involved in the experimental determination of χ parameter, (b) complexities in analyzing the nonlinear failure surface, (c) inexistence of an unique relationship between χ and the volumetric parameter (e.g. S_r), and (d) lack of reliability in considering ψ as a material-independent stress-state variable. Considering these

shortcomings, Lu and Likos (2004) emphatically advocated shifting the entire paradigm into a new three-dimensional framework by replacing the matric suction with *suction stress* (σ^s).

1.3.5 Introduction of Suction stress

Suction stress, the fundamental stress state variable, is the key through which the unsaturated soil property functions are induced within the soil. Based on the thermodynamic principle, Lu et al. (2010) developed the following closed-form expression of suction stress:

$$\sigma^s = -(u_a - u_w) \qquad u_a\text{-}u_w \le 0 \tag{1.6a}$$

$$\sigma^s = -(u_a - u_w) S_e \qquad u_a\text{-}u_w \ge 0 \tag{1.6b}$$

It originates from the combined effect of physicochemical forces, surface tension, and capillarity. Based on suction stress, Lu and Likos (2004) proposed the following effective stress (σ') formulation in the tensorial notation:

$$\sigma'_{ij} = \sigma_{ij} - u_a \delta_{ij} - \sigma^s \delta_{ij} \tag{1.7}$$

Corresponding to the plane strain condition, Equation (1.5) can be further rewritten in the following decoupled form of matrices:

$$\begin{bmatrix} \sigma'_{xx} & \tau'_{xz} \\ \tau'_{zx} & \sigma'_{zz} \end{bmatrix} = \underbrace{\begin{bmatrix} \sigma_{xx} - u_a & \tau_{xz} \\ \tau_{zx} & \sigma_{zz} - u_a \end{bmatrix}}_{\text{Net Normal Stress Tensor}} + \underbrace{\begin{bmatrix} \sigma^s & 0 \\ 0 & \sigma^s \end{bmatrix}}_{\text{Isotropic Suction Stress Tensor}} \tag{1.8}$$

In terms of the suction stress, the shear strength equation becomes to be:

$$\tau_t = c' - \sigma^s \tan\phi' + (\sigma - u_a)\tan\phi' \tag{1.9}$$

Figure 1.3b shows the schematic diagram of the yield plane in the new three-dimensional stress space ((τ–(σ– u_a)–ψ).) One can observe that the conventional nonlinear failure surface

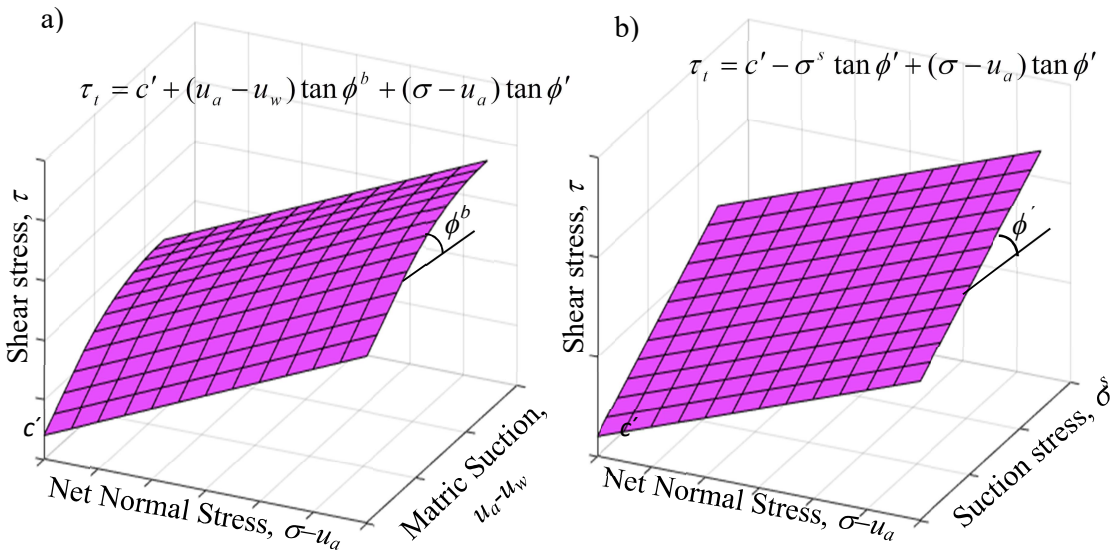

Figure 1.3 The matric suction profile in three-dimensional, a) $\tau - \psi - (\sigma - u_a)$, and b) $\tau - \sigma^s - (\sigma - u_a)$ spaces.

in the new three- dimensional space system gets converted into a planar surface because the frictional strength component on both the stress planes becomes equal and no longer remains the function of the spatial coordinate. This advantage is achieved solely by incorporating suction stress, independent of overburden pressures or external loadings. Considering suction stress as the stress state variable facilitate in turning the variable slope angle (ϕ^b) into a constant one. This provides a high level of computational flexibility.

1.4 BRIEF OUTLINE OF THESIS

The basic limit theorems are used and a few modifications are carried out to formulate (a) an axisymmetric lower bound (LB) FELA technique in conjunction with nonlinear optimization and second-order differentiable yield criterion, and (b) a plane strain upper bound (UB) FELA technique to incorporate the effect of spatially (in later part temporal too)-dependent matric suction in the vadose zone. Using the LB-FELA

technique, a series of analyses are conducted to understand the effect of underlying geo-materials (soils/rocks) and the applied loading arrangements on the ring footing. The LB collapse load is obtained under the purview of saturated soil mechanics. The failure of drained sands, undrained clays, and rocks are modelled with the usage of Mohr–Coulomb, Tresca, and Generalized Hoek–Brown criteria, respectively.

The proposed UB-FELA technique is used to study the load-bearing capacity of strip footing on unsaturated soils considering different loading configurations. The effects of steady-state and transient flow in the vadose zone are thoroughly investigated. The suction stress-based modified Mohr-Coulomb criterion is used to realize the yield behaviour of the unsaturated stratum. The unsaturated property functions are duly incorporated into the analysis by the employment of widely-used soil water characteristics curves and the hydraulic conductivity functions. The underlying geomaterials beneath the foundation are idealized as perfectly plastic and governed by the associative flow rule.

1.5 ORGANIZATION OF THE THESIS

This thesis consists of ten chapters. The current chapter contributes the motivation and overview of research work accomplished in the thesis.

Chapter 2 gives a review of literature related to the limit analysis, bearing capacity of ring footing and the bearing capacity of strip footing resting on unsaturated soil.

Chapter 3 includes the lower bound finite element limit analysis formulation for solving axisymmetric geomechanics problems. The formulation has been elaborately illustrated by considering the hoop stress, 3D yield criteria and nonlinear optimization. The smoothening operations on the representative yield criteria are thoroughly described.

For numerical verification, bearing capacity factor for circular piles embedded in clays are dealt with.

In Chapter 4, the improvement of inclusion of a sandy layer between the ring footing and undrained, cohesive soil is investigated and presented in terms of efficiency factor. An extensive parametric study is conducted to verify the effect of the layer strength, annular section size, top layer thickness, and soil-footing interface conditions.

Chapter 5 focuses on determining the normalized bearing capacity of a ring footing placed over layered soils and subjected to various partial loadings. The study considers three different load positions: inner half, outer half, and middle half loading. The chosen layering configuration of soil strata are: (a) sand on sand, (b) clay on clay, and (c) sand on clay. The effect of loading positions on the strength characteristics are critically scrutinized by considering a wide range of soil strength, ring geometry, layer thickness, surcharge.

Chapter 6 examines the effect of partial loading on the load bearing capacity of ring footing resting on rock mass. The yielding of rock medium is assumed to be dictated by the C^2 continuous Generalized Hoek–Brown criterion. Three different patterns of partial loadings (inner half, middle half, and outer half) have been considered and their effects have been duly investigated by extensively varying the rock strength, overburden pressure, and ring geometry.

Chapter 7 initially proposes a modified upper bound finite element analysis to incorporate the unsaturated state of soil above the ground water table. Thereafter, a detailed study is carried out to evaluate the bearing capacity of strip footing resting on unsaturated sandy soil. The modification is carried out by employing suction stress based Mohr–Coulomb criteria, van Genuchten SWRC model, Darcy's linear flow law, and Gardner's hydraulic conductivity function. The effects of water table positions, soil

strength parameters, and hydromechanical soil properties have been thoroughly investigated.

Chapter 8 focuses on the determination of the ultimate load bearing capacity of strip foundations placed on unsaturated sands and subjected to eccentric and/or oblique loading. The chapter presents a comprehensive investigation that includes the effects of water-table fluctuations, flow conditions, hydromechanical soil properties, loading direction, and the application point of the load. To aid in understanding these effects, a series of numerical simulations are carried out and the bearing capacity charts are developed accordingly. Additionally, nodal velocity contours are generated for specific cases to provide further insights into the behavior of the foundation system.

Chapter 9 describes the unsaturated bearing capacity of strip footing by considering Richard's one- dimensional transient flow. The time-dependent bearing capacity charts are prepared by duly factoring the effect of infiltration rate and duration.

Chapter 10 gives a brief summary and the conclusions from the thesis and discusses the future scope.